Scholar Publishing Group
Nature Environmental Protection
https://doi.org/10.38007/NEP.2020.010204
ISSN 2790-2684 Vol. 1, Issue 2: 27-37

Animal Comfort Studies in Natural Environment Reserves Integrating RS and GIS

Firuz Suleymanov*

Department of Agriculture, University of Ioannina, Kostakii Campus, 47100 Arta, Greece

**corresponding author*

Keywords: Remote Sensing, Geographic Information Systems, Natural Environment Reserves, Animal Comfort

Abstract: Animals are an important part of the natural ecosystem, man's closest friend, an important source of wealth for human society, and a key factor in maintaining ecological balance and the harmonious development of human society. The composition of a fauna includes species composition, relative abundance and species diversity. In order to study the response of faunal communities to environmental change, it is necessary to first understand the species diversity of these communities, to observe the temporal dynamics of species composition and species richness, and to analyse the changing factors affecting the diversity of disturbed communities. The main objective of this paper is to develop a study of animal amenity in natural environmental reserves using RS and GIS techniques. In this paper, seven factors were selected to determine the influence of each natural factor and the parameters of the factors using the frequency of occurrence of animal trace points, to establish a suitable evaluation system using hierarchical analysis, and to evaluate the suitability of the protected areas before and after respectively. The impact on animal habitats is analysed by comparing the approximate distribution of damaged areas using classification. In this paper, the road factor evaluation of suitable areas for animals in nature reserves was graded and statistical analysis of the area was carried out to obtain statistics on the area of suitable areas for animals in nature reserves based on the road factor. The results show that 56.34% of the total area of the reserve is suitable for animals based on the road factor, 14.75% is sub-suitable and 28.91% is unsuitable.

1. Introduction

Faunal composition is strongly influenced by increasing environmental pressures from continued socio-economic development and increased anthropogenic disturbance. The responses of animal species to habitat degradation, including habitat fragmentation and adaptation of small-scale animal populations to anthropogenic disturbance, as well as mechanisms of adaptation at a larger scale (e.g. climate change) will be studied [1, 2]. Habitat loss and fragmentation is a cumulative process that

changes over time. Human activities, such as deforestation and logging, can lead to degradation of forest resources and fragmentation of forest ecosystems. Therefore, in order to conserve forest resources and critical areas, it is important to study the loss and fragmentation of forest habitats due to human activities, as well as the response of animals to changes in light of changes in the composition of forest fauna [3, 4].

In a related study, Mahdi et al. focused on a smart agriculture application that aims to significantly reduce production losses by creating virtual fences that use computer vision and ultrasound emissions to protect crops from hoofed attacks [5, 6]. Starting with an innovative device capable of generating ultrasonic waves to repel hoofed animals and thus protect crops from their attacks, this work provides a comprehensive description of the design, development and evaluation of a smart animal exclusion system that allows the detection and identification of hoofed creatures and the generation of ultrasonic signals appropriate for each hoofed species. Experimental results show that intelligent animal exclusion systems are feasible by deploying animal detectors on power-efficient edge computing devices without compromising average accuracy and meeting real-time requirements.Shalini examined the relationship between empathic design, animal protection poster design and symbolic communication patterns [7, 8]. This was followed by a self-analysis of participant posters to develop a model of the 'designer encoding' to 'audience decoding' framework and to improve the design of self-artwork. Finally, the reliability of the proposed model was verified by testing the questionnaire on 11 groups of animal protection posters. The study culminates in the development of a 'designer-coded' to 'audience-decoded' architectural model for the implementation of animal protection posters, which is in line with the principles of empathic design.

This paper uses a maximum likelihood approach to classify land use/cover in nature reserves based on remotely sensed data, and uses a transfer matrix to study changes in feature class cover, with a focus on vegetation destruction in protected areas [9, 10]. In this paper, the suitability of animal habitats in nature reserves is evaluated. Seven factors were selected: elevation, slope, slope direction, water system, vegetation cover, staple bamboo, and human activities. The frequency of occurrence of animal trace points was used to determine the influence of each natural factor on animal life and to determine the natural factor parameters, and the vegetation index was used to study the changes in vegetation cover of the Sen before and after. A suitable evaluation system was established using hierarchical analysis, and the suitability of the protected areas before and after was evaluated separately. This paper also analyses the impact on animal habitats. The distribution and area changes of suitable habitats for animals before and after the analysis were compared, and the approximate distribution of the damaged areas was analysed using the classification comparison, and the impact on animal habitats was analysed.

2. Design Research

2.1. 3S Technology

RS, or remote sensing technology, is frankly the use of satellites to acquire remote sensing images, which are provided to GIS as macro information and are one of the important data sources for GIS [11, 12].

GIS, on the other hand, is to mine and develop the acquired data (RS data, GPS data, map data, etc.) to extract useful information and apply it in practice [13, 14].

Both are one of the 3S technologies. The connection can be said that RS uses satellites to acquire remote sensing images, which then provide a data source for GIS. The two can be used together, with RS detecting objects and then representing them better through the parsing capabilities of GIS. In fact, RS itself works similarly to an expression, except that it does not have a parsing function,

which users often need to see in order to be practical. Therefore, the two are combined at the same time.

The 3s technology also includes a GPS, which is mainly used for positioning. An example of a strongly expressed relationship is a disaster situation, where information needs to be obtained in time to analyse the location of the rescue and locate the rescue, the application rs senses a disaster situation in an area, reflects it in time, then through analysis, gets the location of the rescue and calculates the rescue area, points etc., and finally uses the gps to locate the rescue. As with RS, it can also be said that GPS provides the data source for GIS [15, 16].

The following diagram can briefly illustrate the relationship between the two

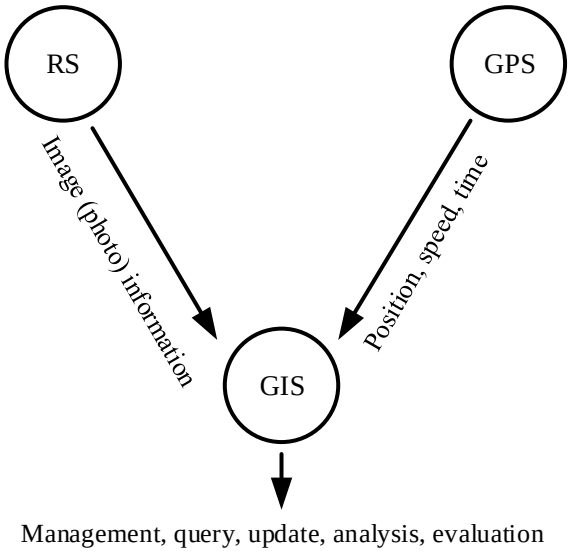

Figure 1. 3S technology interrelationship analysis diagram

2.2. Waveband Preference

As the wavelength range of each band of remote sensing images is different, each band exhibits its unique characteristics. Choosing a suitable combination of bands can effectively remove redundant bands, reduce the amount of computation and improve the computation speed [17, 18]. In this paper, for Landsat5TM image data, the six bands (excluding the sixth thermal infrared band) were used to determine the best band combination by using the statistical matrix method of band correlation.

Table 1. TM image band correlation coefficient matrix

	Band1	Band2	Band3	Band4	Band5	Band7
Band1	1					
Band2	0.863417	1				
Band3	0.595346	0.911515	1			
Band4	0.033286	0.458453	0.763982	1		
Band5	0.604159	0.403244	0.12945	0.342705	1	
Band7	0.563791	0.363476	0.091812	0.337268	0.988433	1

The value of the correlation coefficient reflects the degree of correlation of the linear relationship between the two bands. The smaller the correlation coefficient, the higher the independence between the two bands and the less redundant information. The correlation coefficients of the two

shortwave infrared bands are the highest, reaching over 0.98, indicating that the spectral coherence of these two bands is high and there is a lot of redundant information, so it is not suitable to appear in a band combination at the same time; the correlation coefficients of the visible bands (Band1, Band2, Band3) are relatively large, all above 0.5, and there is also more redundant information, so in practice the visible bands may be used in a The two bands with the smallest correlation coefficients are Band1 and Band4, which indicate that the two bands are independent and have a large amount of information.

In this paper, the optimal index factor (OIF) method is used to calculate the optimal index factor of the waveband combination of remote sensing images. Its calculation formula is as follows.

$$OIF = \frac{\sum_{i=1}^{n} S_i}{\sum_{i=1, j=1}^{n} |r_{i,j}|} \tag{1}$$

where Si is the standard deviation and ri,j denotes the correlation coefficient between the bands. the larger the OIF index, the greater the information content and the smaller the correlation between two. Table 2 shows the OIF values for 20 combinations of the six bands of TM images.

$$C = 1 - \sum (\frac{Ni}{N})^2 \tag{2}$$

From the OIF values in the table, it can be seen that the largest OIF value is 526.54301 for the combination of bands 1, 4 and 7. This combination is also consistent with the previous analysis of the correlation coefficients between the bands in Table 1. Therefore, 147 is used as the optimal band combination for TM5 images.

The band combination of 257 was chosen for Landsat8 because of the similarity between the band combinations of Landsat8 and TM images.

2.3. Data Analysis and Processing Methods

1) Analysis of faunal community structure in protected areas

Based on the fact that animal resources are the most abundant among all animal resources, the diversity index was used to measure the animal diversity, community dominance and density of the reserve based on the results of the survey in the sample line.

(1) Animal diversity was measured using the Shannon-Wiener diversity index. Calculation formula.

$$H' = \sum_{i=0}^{s} Pil \log_2 Pi \tag{3}$$

H' refers to the diversity index; S refers to the number of species; Pi refers to the proportion of individuals.

(2) Animal community dominance was calculated using the Simpson dominance index. Calculation formula

$$C = 1 - \sum (\frac{Ni}{N})^2 \tag{4}$$

C refers to the dominance index; Ni refers to the number of individuals; N is the total number of

individuals

(3) Animal community density was calculated using Distance 6.0 software based on the species and numbers recorded in the sample line survey and according to the vertical distance of the sample line.

3. Experimental Study

3.1. Analysis of Changes in the Landscape Pattern of Protected Areas

1）Landscape scale and patch data acquisition

For the analysis of landscape pattern changes in animal nature reserves, the acquired satellite images of the reserves need to be interpreted and processed by remote sensing information. The processing of remote sensing images is carried out in the following seven steps (see Figure 2). The remote sensing images used in this study were based on Landsat TM images of three different years, supplemented by field survey data, and the landscape index method was used to interpret the images of the whole reserve and analyse the change in landscape pattern between the current and past years. The landscape changes of the protected area were analysed in the past. At the same time, the relationship between faunal resources and landscape change was analysed according to the process of landscape pattern change in the reserve.

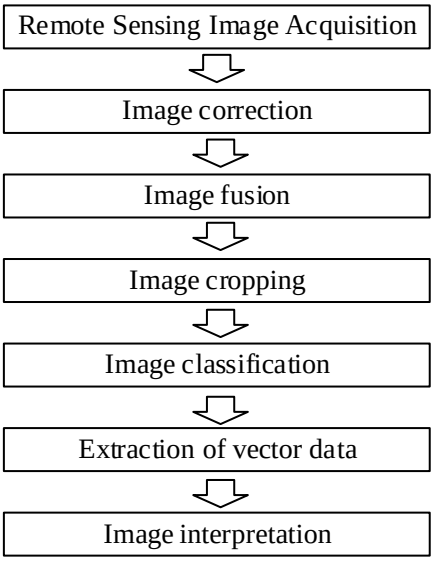

Figure 2. Remote sensing image processing steps

(2) Classification of landscape elements and selection of landscape indices

It is a prerequisite for the interpretation of satellite images to clarify the types of landscape elements in the reserve and to classify them reasonably, which is helpful for the extraction of different samples in the process of image interpretation. Firstly, different wavebands were selected and the satellite images were processed with Erdas Imagine 9.2 software for optimal waveband combination, image enhancement and cropping of the study area, and an evaluation template was established according to the classification criteria and types required for the study. Secondly, with the help of Arc Gis 9.3 software, an interactive image interpretation of the landscape type map of the study area was carried out and the processed vector files were output; finally, Fragstats 4.2 software was used to calculate landscape indices and landscape patches for the vector files of the landscape type layer of remote sensing images of the study area.

3.2. Nature Reserve Animal Habitat Suitability Evaluation

Based on the remote sensing image data, the vegetation cover of the animal nature reserve was analysed, and the distribution of animal trace points was used as the main clue to carry out statistical analysis of its natural factors such as elevation and slope, and combined with the distribution of human activities and animal staple bamboo, the habitat suitability evaluation system of the nature reserve was established, based on which the habitat suitability area of the reserve was analysed in recent years.

Firstly, the vegetation cover was extracted.

The degree of vegetation cover reflects the degree of lushness of the vegetation. As an important parameter for characterising the vegetation cover on the ground, it has important applications in climate, hydrology and soil research. Remote sensing technology has become an important tool for vegetation cover extraction due to its advantages in large-scale observation and high continuous capability. As there is an obvious linear relationship between vegetation cover and NDVI, vegetation cover can be estimated by establishing a conversion relationship and binning the image data. The principle of this method is to split an image element into two parts. Assuming that each image element consists of vegetation and non-vegetation information, the NDVI value of that image element must also consist of these two components, which can be expressed as

$$NDVI = NDVI_{soil} \bullet (1 - f_{veg}) + NDVI_{veg} \bullet f_{veg} \tag{5}$$

where: NDVI soil is the non-vegetation NDVI value, NDVI veg is the vegetation NDVI value, and f veg is the degree of coverage. Therefore, the formula for vegetation cover can be deduced from Equation 4 as

$$f_{veg} = \frac{NDVI - NDVI_{soil}}{NDVI_{veg} - NDVI_{soil}} \tag{6}$$

Therefore the value of NDVI veg and NDVI soil becomes the key to obtain the vegetation cover. Some scholars have transformed the problem of solving NDVI veg and NDVI soil into the determination of the four parameters of maximum cover, minimum cover, maximum NDVI and minimum NDVI in the study area, and pointed out that when the minimum cover in the study area can be approximated as 0 and when the maximum cover can be approximated as 1, a confidence interval can be given to the NDVI value, so as to obtain the maximum and minimum NDVI values in the interval. In this case, NDVI soil = NDVI min and NDVI veg = NDVI max, which is used to calculate the vegetation cover of the study area.

The study area is a nature reserve and there are approximately pure bare ground and pure vegetation images in the area, so this is the case. This paper uses a confidence interval of 5% to 95% for the NDVI values and extracts the vegetation cover using the NDVI.

4. Experiment Analysis

4.1. Analysis of the Protected Area Landscape Aggregation and Dispersion Index

Agglomeration (AI) refers to the degree of aggregation of different landscape elements or the dispersion of landscape patches over the overall landscape, and is used to measure the maximum possible degree of proximity of elements in the composition of a landscape. The higher the Aggregation Index, the better the connectivity of a particular landscape type; conversely, a tight arrangement of elements in the landscape indicates a high degree of landscape fragmentation. In particular, Table 3 analyses the aggregation index over a 25-year period.

Table 3. Annual aggregation index AI (%) for animal nature reserves over 25 years

	Type of plaque				
Year	Woodland	Arable land	Building	Roads	Landscape level
1	85.53	50.76	11.82	19.35	77.26
12	76.46	59.81	24.26	16.29	67.80
25	79.87	53.16	31.43	27.49	67.43

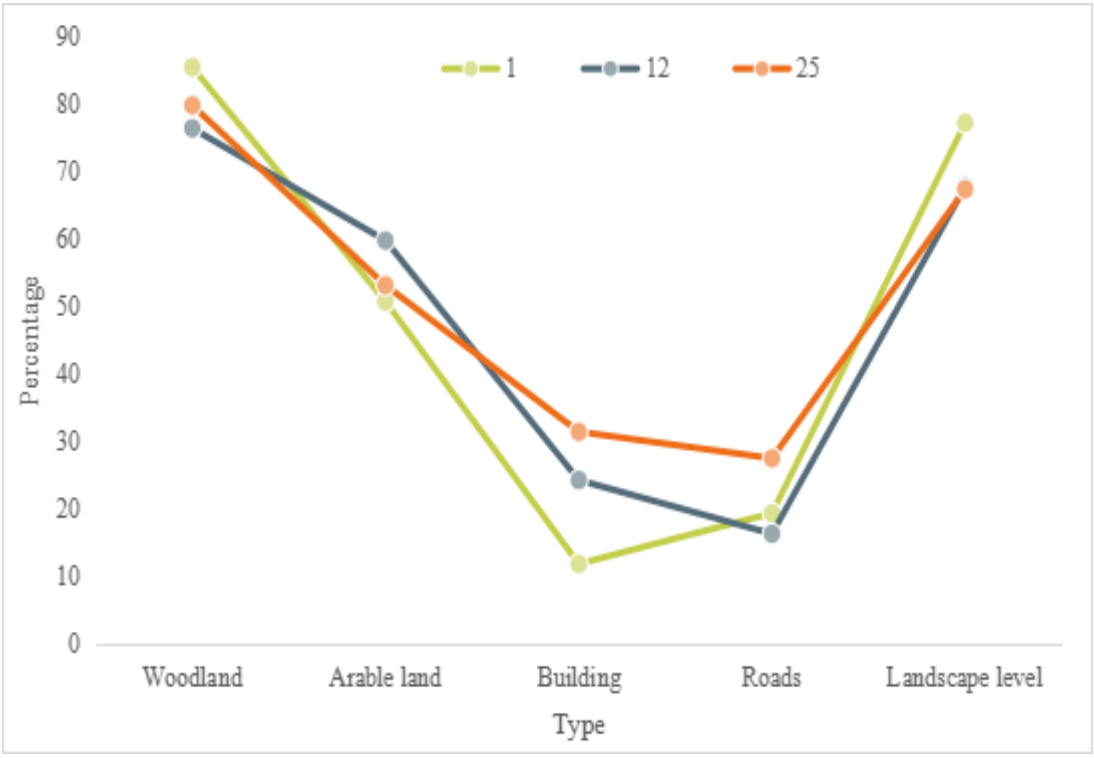

Figure 3. Analysis of the annual aggregation index of animal nature reserves over a 25-year period

In terms of patch type, the AI index of aggregation of forested land is the highest in all years, indicating that forested land has the highest degree of inter-patch connectivity, which has positive significance for the development of the reserve; the AI index of aggregation of cultivated land reaches the highest in the 12th year, indicating that there is more cultivated land and aggregation in this period, with the increase of migrant workers in the reserve, the original cultivated land becomes abandoned land, and after the implementation of the policy of returning cultivated land to forest in the reserve, it is gradually replaced by some vegetation, and its AI index shows a decreasing trend in the 25th year. The AI index of the reserve has gradually been replaced by some vegetation, and its AI index shows a decreasing trend in the 25th year. The AI of the aggregation indices of buildings and roads both show an increasing trend as the years go by, indicating that the distribution of construction land patches in the reserve tends to become more concentrated, and the connectivity of roads is also getting higher. In terms of landscape level, the overall aggregation index of the reserve shows a decreasing trend, from 77.26% in the first year to 67.80%, indicating that the aggregation and connectivity among the landscape elements of the reserve gradually weaken and the landscape shows a fragmentation trend (Figure 3).

4.2. Vegetation Cover Classification

By using GIS analysis, the vegetation cover in the study area was divided into five classes, with each 0.2 being a class, and the area was counted, and the statistical results are shown in Table 4.

Table 4. Statistics on changes in vegetation cover in the study area over a 5-year period

Vegetation cover	First year	Fifth year
0-20%	27.25%	31.48%
20%-40%	16.94%	26.10%
40%-60%	18.88%	13.71%
60%-80%	15.92%	27.30%
80%-1	21.01%	7.41%

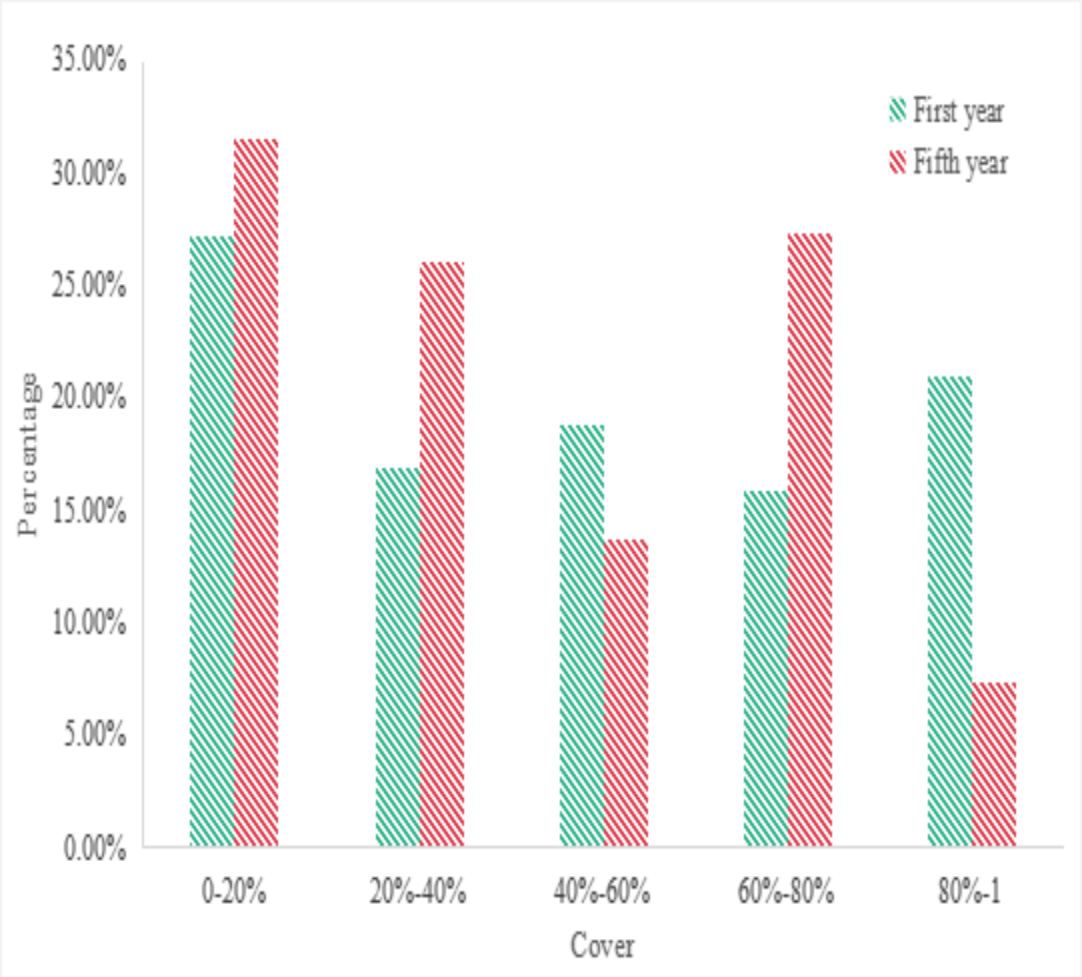

Figure 4. Analysis of changes in vegetation cover in the study area over a 5-year period

An analysis of the vegetation cover statistics for the two time periods in Figure 5 shows that the vegetation cover in the study area is decreasing dramatically, with the area with 40% or more cover being 55.81% in the first year and 48.52% in the fifth year, a decrease of 7.92% in five years. In particular, the area with 80% or more vegetation cover has decreased by 14.6%. This shows that the vegetation cover of the nature reserve has been seriously damaged in the five years.

4.3. Human Activity Factors

The human activity factor involved in this paper is the road factor, by vectorising the road information from the previous data preparation work in ArcGIS for buffer zone analysis. According to the evaluation guidelines, the road factor was evaluated by using 500m as the threshold value, and areas greater than 500m from the road were considered suitable areas, while areas less than 500m were considered unsuitable areas, and the statistical analysis of the area was carried out to obtain the statistics of the area of suitable living areas for animals in the nature reserve based on the road factor.

Table 5. Statistics on the area of suitable living areas for animals in nature reserves based on road factors

Suitability	Road distance (m)	Percentage of area
Suitability	>800	56.34%
Sub-suitable	500-800	14.75%
Unsuitable	<500	28.91%

The statistical table of road factors for nature reserves shows that 56.34% of the total area of the reserve is suitable for animals based on road factors, 14.75% is sub-suitable and 28.91% is unsuitable.

5. Conclusion

The experiments in this paper have analysed the suitability of animal habitats based on several factors, and although some conclusions and results have been obtained, there are still several problems: firstly, the selection of habitat factors. In this paper, only one factor, forest cover, was used in the selection of biological factors, which is too few. Other habitat factors such as soil, vegetation species, forest biomass etc. should be taken into account. In this study, due to the limitations of the content and project technology, other biological factors than vegetation cover and staple bamboo were not addressed. Therefore, the selection of suitable evaluation factors and the establishment of a more reasonable and scientific evaluation system will be the direction of future research. The second is the selection of remote sensing data sources. Compared with the development of remote sensing technology in terms of the spatial resolution of remote sensing images, the classification of remote sensing image information at this scale can be said to be not good enough to classify land types. The third is the classification method. Only the maximum likelihood method was used to operate on the classification of the images, and no comparison was made under multiple methods.

Funding

This article is not supported by any foundation.

Data Availability

Data sharing is not applicable to this article as no new data were created or analysed in this study.

Conflict of Interest

The author states that this article has no conflict of interest.

References

[1] Busra Tegin, Eduin E. Hernandez, Stefano Rini, Tolga M. Duman. Straggler Mitigation Through Unequal Error Protection for Distributed Approximate Matrix Multiplication. IEEE J. Sel. Areas Commun. (2020) 40(2): 468-483.

[2] Astha Chawla, Animesh Singh, Prakhar Agrawal, Bijaya Ketan Panigrahi, Bhavesh R. Bhalja, Kolin Paul. Denial-of-Service Attacks Pre-Emptive and Detection Framework for Synchrophasor Based Wide Area Protection Applications. IEEE Syst. J. (2020). 16(1): 1570-1581.

[3] Vivek Kumar Singh, Manimaran Govindarasu. A Cyber-Physical Anomaly Detection for Wide-Area Protection Using Machine Learning. IEEE Trans. Smart Grid. (2020) 12(4): 3514-3526.

[4] Tamara Becejac, Crystal Eppinger, Aditya Ashok, Urmila Agrawal, James O'Brien. PRIME: A Real-Time Cyber-Physical Systems Testbed: from Wide-Area Monitoring, Protection, and Control Prototyping to Operator Training and Beyond. IET Cyper-Phys. Syst.: Theory & Appl. (2020) 5(2): 186-195. https://doi.org/10.1049/iet-cps.2019.0049

[5] Mahdi Haghifam, M. Nikhil Krishnan, Ashish Khisti, Xiaoqing Zhu, Wai-Tian Tan, John G. Apostolopoulos. On Streaming Codes With Unequal Error Protection. IEEE J. Sel. Areas Inf. Theory. (2020) 2(4): 1165-1179.

[6] Bokka Krishna Chaitanya, Anamika Yadav, Mohammad Pazoki. Wide Area Monitoring and Protection of Microgrid with DGs Using Modular Artificial Neural Networks. Neural Comput. Appl. (2018) 32(7): 2125-2139. https://doi.org/10.1007/s00521-018-3750-4

[7] Shalini, Subhransu Ranjan Samantaray. A Differential Voltage-Based Wide-Area Backup Protection Scheme for Transmission Network. IEEE Syst. J. (2020) 16(1): 520-530.

[8] Sima Ghafoori, Ahmad Shalbaf. Predicting Conversion from MCI to AD by Integration of Rs-Fmri and Clinical Information Using 3D-Convolutional Neural Network. Int. J. Comput. Assist. Radiol. Surg. (2020) 17(7): 1245-1255.

[9] Mateusz Marcisz, Margrethe Gaardløs, Krzysztof K. Bojarski, Till Siebenmorgen, Martin Zacharias, Sergey A. Samsonov. Explicit Solvent Repulsive Scaling Replica Exchange Molecular Dynamics (RS-REMD) in Molecular Modeling of Protein-Glycosaminoglycan Complexes. J. Comput. Chem. (2020) 43(24): 1633-1640. https://doi.org/10.1002/jcc.26965

[10] Niklas Sülzner, Julia Haberhauer, Christof Hättig, Arnim Hellweg. Prediction of Acid Pka Values in the Solvent Acetone Based on COSMO-RS. J. Comput. Chem. (2020) 43(15): 1011-1022. https://doi.org/10.1002/jcc.26864

[11] Leonel Mera-Jiménez, John F. Ochoa-Gómez. Volume Reduction Techniques for the Classification of Independent Components of rs-fMRI Data: A Study with Convolutional Neural Networks. Neuroinformatics. (2020) 20(1): 73-90.

[12] Savita Soma, Mahesh V. Sonth, Sanjaykumar C. Gowre. Design of Two-Dimensional Photonic Crystal Based Ultra Compact Optical RS Flip-Flop. Photonic Netw. Commun. (2020) 43(2): 109-115.

[13] Arjun BS, Alekya B, Hari RS, Vikas V, Anita Mahadevan, Hardik J. Pandya. Electromechanical Characterization of Human Brain Tissues: A Potential Biomarker for Tumor Delineation. IEEE Trans. Biomed. Eng. (2020) 69(11): 3484-3493.

[14] Kamal Rsetam, Zhenwei Cao, Zhihong Man. Design of Robust Terminal Sliding Mode Control for Underactuated Flexible Joint Robot. IEEE Trans. Syst. Man Cybern. Syst. (2020) 52(7): 4272-4285.

[15] Kevin Weinberger, Alaa Alameer Ahmad, Aydin Sezgin, Alessio Zappone. Synergistic Benefits in IRS- and RS-Enabled C-RAN With Energy-Efficient Clustering. IEEE Trans. Wirel. Commun.

(2020) 21(10): 8459-8475.

[16] Hyunwoo Cho, Hong-Yeop Song, Jae-Min Ahn, Deok Won Lim. Some New RS-coded Orthogonal Modulation Schemes for Future GNSS. ICT Express. (2020) 7(4): 530-534.

[17] Akhilesh Yadav, Poonam Jindal, Devaraju Basappa. Design and Implementation of RS(450, 406) Decoder: Forward Error Correction by Reed Solomon Decoding. Int. J. Embed. Real Time Commun. (2020) Syst. 12(1): 19-43.

[18] Banu Yetkin Ekren. A Multi-Objective Optimisation Study for the Design of An AVS/RS Warehouse. Int. J. Prod. Res. (2020) 59(4): 1107-1126. https://doi.org/10.10 80/00207543.202 0.17 20927